PERGAMON

International Journal of Solids and Structures 39 (2002) 1307–1326

INTERNATIONAL JOURNAL OF SOLIDS and STRUCTURES

www.elsevier.com/locate/ijsolstr

A structural model for high pressure helical wire-wound thermoplastic hose

J.J. Evans *, P.D. Wilcox

Department of Mechanical Engineering, Imperial College of Science Technology and Medicine, South Kensington, London SW7 2BX, UK

Received 17 January 2001; received in revised form 25 July 2001

Abstract

This paper develops a model for a specific type of hose construction designed to withstand very high operating pressures. The model is based on a model previously developed by Entwistle and White (Int. J. Mech. Sci. 19 (1977) 193) with two significant modifications. Firstly the compressible inner core is included in the model using Lamé's thick walled cylinder theory. Secondly the model allows for the squeezing effect on wires when a hose gets shorter under pressurisation. The model calculates whether the wires in a particular layer will be squeezed together and when this occurs, the behaviour is modelled using Hertzian contact theory. The governing equations are solved using a minimising Newton Raphson technique. Model predictions are compared with experimental results obtained for pressure deformation response in terms of hose axial strain and wire strain and show good agreement. Considerable hysteretical behaviour is seen in the hose axial strain and it is suggested that this may be due to the twisting contact movements between different layers and as such may be a good indicator of the amount of fretting taking place. It is also suggested that, when a hose is designed to get shorter on pressurisation, length change may be a good indicator of manufacturing quality in terms of wire packing efficiency.

Keywords: Hose; Wire; Strain gauges; Strand

1. Introduction

Thermoplastic wire hoses used in a number of contemporary high pressure applications have a significantly different construction to standard rubber hoses (SAE J517, 1986). Some applications include water jet cutting and blasting (Raghaven and Olsen, 1989), oil well blow out preventers and bolt tensioning devices (Anon, 1992).

The hoses consist of an inner thermoplastic core with layers of wires wound around it. The wire layers are wound in pairs, one layer of each pair being wound left hand and the other right hand in order to

* Corresponding author. Current address: Department of Engineering, University of Reading, Whiteknights, Reading RG6 2AY, UK. Tel.: +44-1189-875-123; fax: +44-118-931-8923.

E-mail address: j.j.evans@rdg.ac.uk (J.J. Evans).

0020-7683/02/$ - see front matter
PII: S0020-7683(01)00201-3

Nomenclature

A_i	wire area of one wire in layer
d_i	wire diameter in layer
d_{sp}	available space for wire
E_i	Young's modulus of wires in layer
E_{ic}	Young's modulus of the inner core
F_a	hose axial force caused by wire squeezing
F_L	lateral force caused by wire squeezing (in its own axis)
F_{LU}	lateral force per unit length caused by wire squeezing (in its own axis)
F_R	radial force caused by a helical wire in tension
F_{RU}	radial force per unit length caused by a helical wire in tension
F_{zic}	axial force contribution of the inner core
G_i	modulus of rigidity of a wire
l_i, l_i'	wire length in one pitch of helix of layer
S_i	pitch length of a wire layer (axial length of one rotation of helix)
N_i	number of wires in layer
n	number of layers in a particular construction of hose
P_0, P_i	internal pressure, interlayer pressure on inside of layer
R_i, R_i'	inner winding radius of layer
T_a, T_i	axial tension in a strand, axial tension in a wire of layer
Greeks	
α_i, α_i'	lay angle of helix of layer
γ_i	twist coefficient in a single pitch of a helix
ε_i	wire strain
ε_z	hose axial strain
ε_{li}	lateral wire strain in layer
ν_{ic}	Poisson's ratio of the inner core
$\xi_i[\varepsilon_{li}]$	parameter for wire compression theory in layer (which is a Boolean function of the lateral wire strain)
ρ, ρ_c	radius and complimentary radius of curvature of a helix
Indices	
$(')$	denotes pressurised state
i	subscript denotes that the parameter refers to reinforcement layer i

achieve a torque balanced construction (i.e. minimal twist on pressurisation). There are no intermediate layers of plastic and wires in the same layer are touching in order to maximise packing density. On the outside of the reinforcement layers is a thermoplastic outer cover which mainly serves to protect the reinforcement from wear or corrosion. The hoses are often designed to get shorter on pressurisation as this has been found to improve their endurance. The details of hose constructions used in this work are given in Tables 1–7. The ability to predict the mechanical behaviour of these hoses will allow hose designers to optimise their designs for load sharing between reinforcement layers. It will also give an insight into the mechanisms of fatigue and allow design changes to improve the endurance characteristics.

Table 1
Two layer hose inner core data and hose burst pressure

Hose	Material	R_0 (mm)	R_1 (mm)	v_{ic}	E_{ic} (MPa)	Burst (bar)
2006st	PA12	3.15	4.15	0.47	350	2100
2006str	POM	3.15	4.05	0.4	2900	2250
2012st	PEE5556	6.4	7.55	0.47	350	1400

Table 2
Two layer hose wire geometry and material properties

Hose	R_1 (mm)	N_1	A_1 (mm^2)	D_1 (mm)	E_1 (MPa)	α_1 (degrees)
Layer 1						
2006st	4.15	52	0.071	0.3	210000	54.7322
2006str	4.05	42	0.096	0.35	210000	56.3756
2012st	7.55	70	0.126	0.4	210000	54.8996
	R_2 (mm)	N_2	A_2 (mm^2)	D_2 (mm)	E_2 (MPa)	α_2 (degrees)
Layer 2						
2006st	4.45	54	0.071	0.3	210000	55.9095
2006str	4.4	46	0.096	0.35	210000	55.9382
2012st	7.95	71	0.126	0.4	210000	56.3167

Table 3
Four layer hose inner core data and hose burst pressure

Hose	Material	R_0 (mm)	R_1 (mm)	v_{ic}	E_{ic} (MPa)	Burst (bar)
4006st	PA12	3.15	4.05	0.47	350	3500
4012st	PA12	6.4	7.65	0.47	350	3250

Table 4
Four layer hose wire geometry and material properties

Hose	R_1 (mm)	N_1	A_1 (mm^2)	D_1 (mm)	E_1 (MPa)	α_1 (degrees)
Layer 1						
4006st	4.05	42	0.096	0.35	210000	56.3756
4012st	7.65	48	0.283	0.6	210000	54.7910
	R_2 (mm)	N_2	A_2 (mm^2)	D_2 (mm)	E_2 (MPa)	α_2 (degrees)
Layer 2						
4006st	4.4	46	0.096	0.35	210000	55.9382
4012st	8.25	49	0.283	0.6	210000	56.8201
	R_3 (mm)	N_3	A_3 (mm^2)	D_3 (mm)	E_3 (MPa)	α_3 (degrees)
Layer 3						
4006st	4.75	49	0.096	0.35	210000	56.3434
4012st	8.85	64	0.246	0.56	210000	51.3350
	R_4 (mm)	N_4	A_4 (mm^2)	D_4 (mm)	E_4 (MPa)	α_4 (degrees)
Layer 4						
4006st	5.1	52	0.096	0.35	210000	56.6932
4012st	9.41	66	0.246	0.56	210000	52.6231

Table 5
Six layer hose inner core data and hose burst pressure

Hose	Material	R_0 (mm)	R_1 (mm)	ν_{ic}	E_{ic} (MPa)	Burst (bar)
6005st	POM	2.4	3.65	0.4	2900	6250
6012st	PA12	6.4	7.65	0.47	350	4500

Table 6
Six layer hose wire geometry and material properties

Hose	R_1 (mm)	N_1	A_1 (mm^2)	D_1 (mm)	E_1 (MPa)	α_1 (degrees)
Layer 1						
6005st	3.65	37	0.096	0.35	210000	57.3954
6012st	7.65	47	0.283	0.6	210000	55.6290
	R_2 (mm)	N_2	A_2 (mm^2)	D_2 (mm)	E_2 (MPa)	α_2 (degrees)
Layer 2						
6005st	4	39	0.096	0.35	210000	58.6442
6012st	8.25	48	0.283	0.6	210000	57.5814
	R_3 (mm)	N_3	A_3 (mm^2)	D_3 (mm)	E_3 (MPa)	α_3 (degrees)
Layer 3						
6005st	4.35	53	0.071	0.3	210000	55.7817
6012st	8.85	62	0.246	0.56	210000	52.7537
	R_4 (mm)	N_4	A_4 (mm^2)	D_4 (mm)	E_4 (MPa)	α_4 (degrees)
Layer 4						
6005st	4.65	56	0.071	0.3	210000	56.1485
6012st	9.41	63	0.246	0.56	210000	54.5873
	R_5 (mm)	N_5	A_5 (mm^2)	D_5 (mm)	E_5 (MPa)	α_5 (degrees)
Layer 5						
6005st	4.95	58	0.071	0.3	210000	57.1120
6012st	9.97	69	0.196	0.5	210000	57.5024
	R_6 (mm)	N_6	A_6 (mm^2)	D_6 (mm)	E_6 (MPa)	α_6 (degrees)
Layer 6						
6005st	5.25	62	0.071	0.3	210000	56.7564
6012st	10.47	72	0.196	0.5	210000	57.6916

Table 7
Hose 8005 inner core and reinforcement data

Core material	R_0 (mm)	R_1 (mm)	ν_{ic}	E_{ic} (MPa)		Burst (bar)
POM	2.25	3.5	0.4	2900		7440
Wires	R_i (mm)	N_i	A_i (mm^2)	D_i (mm)	E_i (MPa)	α_i (degrees)
Layer 1	3.5	19	0.210	0.3	210000	54.5541
Layer 2	3.8	20	0.210	0.3	210000	55.6606
Layer 3	4.1	53	0.071	0.3	210000	53.4569
Layer 4	4.4	56	0.071	0.3	210000	54.0096
Layer 5	4.7	58	0.071	0.3	210000	55.1808
Layer 6	5	62	0.071	0.3	210000	54.9135
Layer 7	5.3	63	0.071	0.3	210000	56.5004
Layer 8	5.6	68	0.071	0.3	210000	55.6217

2. Previous theory

Hose theories have developed along two separate paths according to different types of hose constructions: hose with a low fraction of reinforcement where the rubber within the construction plays a dominant role in the hose behaviour and hose where the wire reinforcement plays a dominant role in the hose behaviour. The theory for rubber dominated hose has been developed predominantly by Kuipers and co-workers (Van Den Horn and Kuipers, 1988; Kuipers and Van der Veen, 1989; Teerling, 1994). Wire dominated hose theories are an extension of wire strand theory (a strand is defined as a number of wires wound helically around a central wire or solid plastic core). A short review of relevant strand and hose theory pertinent to the current theory will be made in the following paragraphs. A more complete discussion and review of strand theory is given by Cardou and Jolicoeur (1997).

Hruska (1951, 1952, 1953) analysed the axial, tangential and radial stresses within a strand assuming no change in the reinforcement winding radius, no twist and no change in lay angle, α. The wires were assumed to have tensile stiffness but no bending or torsional stiffness. The relationship for axial force, T_a, as a function of wire tension T_i, is (where α_i is the lay angle):

$$T_a = T_i \cos \alpha_i \tag{1}$$

Hruska gives an expression for radial force per unit length of a wire as a relationship between the wire tension, T, and radius of curvature, ρ, (a proof for this is given by Machida and Durelli (1973)). In the limit, for a large radius of curvature to unit length ratio, the radial force per unit length, F_{RU}, is given by

$$F_{RU} = \frac{T}{\rho} \tag{2}$$

where the radius of curvature can be shown for a helix to be

$$\rho = \frac{R_i}{\sin^2 \alpha_i} \tag{3}$$

where R_i is the winding radius of the helix (see for example Lord and Wilson (1984)).

A more appropriate assumption for a hose reinforcement geometry is one which allows geometric changes to take place as the hose is pressurised. The first model along these lines was proposed by Entwistle and White (1977) for a rubber braided hose. The geometry of the deformed reinforcement is shown in Fig. 1. The model does not allow twisting of the hose since this will be zero for a braided hose.

The relationships between the wire winding radius in undeformed and deformed conditions can be derived by the trigonometric relations and result in the following expression:

$$\frac{R_i'}{R_i} = (1 + \varepsilon_i) \frac{\sin \alpha_i'}{\sin \alpha_i} \tag{4}$$

The pressure which one layer applies on another can be derived from the radial force per unit length of hose (Eq. (2)), if this is divided by the circumference of the layer it gives a pressure. Although only given for the case for a two layer hose, this can easily be extended to a multiple layer hose with n layers in the form of the summation:

$$P_1 = \sum_{i=1}^{n} \frac{N_i A_i E_i \varepsilon_i \sin \alpha_i' \tan \alpha_i'}{2\pi R_i'^2} \tag{5}$$

The expression for axial equilibrium (extended to multiple layers) is given in the following summation:

$$\pi R_1'^2 P_1 + \pi \sum_{i=1}^{n-1} (R_{i+1}'^2 - (R_i' + d_i)^2) P_{i+1} = \sum_{i=1}^{n} N_i A_i E_i \varepsilon_i \cos \alpha_i' \tag{6}$$

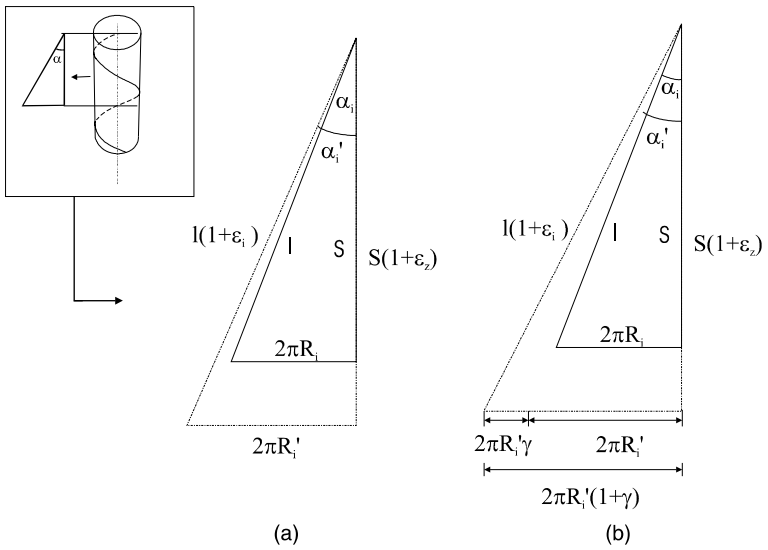

Fig. 1. Assumption for the deformed reinforcement geometry, according to Entwistle and White (1977) and Knapp (1979).

The right-hand side of the equation represents the axial force of the helical wires as proposed by Hruska (Eq. (1)). The left-hand side represents the pressure of the fluid medium acting against the end of the hose, the outer diameter of the inner core is used because the inner core is assumed to have no shear stiffness and behave like an incompressible fluid. This expression is added to a summation which represents the pressure effect of rubber between each pair of reinforcement layers, this was also assumed to act like incompressible fluid. This interlayer expression is slightly different from that given by Entwistle and White (1977), because in this paper the winding radius of a layer, R_i, is defined as the inner diameter (rather than the middle) and because the volume of the wires has not been included here.

Finally the relationship between the winding radius of one layer and the next was determined by the incompressible rubber between them and this was enforced by the following constant volume equation (again this expression is slightly different from Entwistle and White (1977) for the reasons mentioned in the previous paragraph):

$$(\pi R_{i+1}^2 - \pi(R_i + d_i)^2) = (\pi R_{i+1}'^2 - \pi(R_i' + d_i)^2)(1 + \varepsilon_z) \tag{7}$$

Knapp (1979) developed a stiffness matrix for strands with a soft core which allowed for radius changes in the helical wires caused by the compression of the core. It also allowed for the overall twist of the strand (in a similar way to Machida and Durelli (1973)) by a twisting factor γ (see Fig. 1(b)) giving the expression:

$$R_i' = R_i \frac{(1 + \varepsilon_i)\sin\alpha_i'}{(1 + \gamma_i)\sin\alpha_i} \tag{8}$$

Breig (1988) develops a theory which attempts to take into account the twisting effect that a 'spiralised' reinforcement will have on a hose, using the same deformed helical wire geometry as Knapp (1979) (see Fig. 1(b)). Unlike Knapp only the axial strains in the wires are taken into consideration and the torsional effect of the helical wires is derived from the tangential force multiplied by its effective lever arm. The polar second moment of area of a single layer is approximated by a tube with thickness t. The tube is

assumed to have the same thickness as a wire diameter, this gives an expression for the rotation coefficient, γ_i, as follows:

$$\gamma_i = \frac{R_i N_i A_i E_i \varepsilon_i \sin \alpha_i'}{2\pi (R_i' + (d_i/2))^2 d_i G_i \tan \alpha_i} \tag{9}$$

All the other relationships in Breigs' theory follow the same lines as Entwistle and White (1977). After some algebraic manipulations Breig (1988) ends up with a system of $2n$ equations with $2n$ unknowns being $\alpha_{1-n}'\gamma_{1-n}$ with the internal pressure and the axial strain, ε_z, as input parameters. He also presents pressure deformation relationships for an incompressible inner core as follows:

$$R_0' = \left[R_1'^2 - \frac{(R_1^2 - R_0^2)}{(1+\varepsilon_a)} \right]^{1/2} \tag{10}$$

$$P_0 = P_1 + \frac{2E_{ic}}{3} \left[R_1' - R_1 + \frac{R_1 \varepsilon_a}{2} \right] \frac{(R_1^2 - R_0^2)}{R_1 R_0^2} \tag{11}$$

Jakeman and Knight (1995) used the Breig (1988) theory for a thermoplastic hose, but they changed the interlayer compatibility condition to the following:

$$R_{i+1}' = R_i' + 2d_i \tag{12}$$

This is because there was no interlayer of rubber in the hose construction. The expression is $2d$ because the layers are braided and so each layer is $2d$ thick (as it is two sets of wires counter wound). They also added a number of other factors to account for the fact that it is a polymer fibre reinforced hose rather than a wire reinforced hose. These included accounting for the radius of curvature effect on the yarn strength and including the friction at the braid crimp locations in an attempt to account for hysteresis.

2.1. Discussion

No hose theory attempts to model the individual wire bending and twisting effects. There is some justification for this as the relative diameter of the wires in the hose is considerably smaller, as a proportion to the overall structure, compared with that of a seven wire strand.

There are a number of specific criticisms of the Breig (1988) model. Firstly, the assumption that the polar second moment of area is equivalent to a solid tube seems over simplistic and will result in much stiffer behaviour than actually exists, it probably does represent an upper bound to the hose twisting stiffness. An alternative approximate assumption for the polar moment of inertia would be the sum of the individual polar moment of inertia of each wire about its own axis, this would represent a lower bound value. The Breig (1988) model uses the axial strain as an input, yet it is not difficult to rearrange the equations of the model to allow prediction of the axial strain. Since this is one of the few easily measured characteristics of a hose it seems sensible to predict values that can be compared with the experimental results and thus give an indication of the validity of the model. Finally the Breig (1988) numerical solution involves $2n$ unknowns $\alpha_{1-n}'\gamma_{1-n}$ with $2n$ equations. This solution has a parameter for twist, γ, for every layer and yet all the layers in the hose twist together (as shear strain in the rubber interlayers is neglected in this analysis). These parameters could be eliminated in favour of an overall twist parameter and reduce the $2n$ equations down to $n+1$.

3. Development of the model

3.1. Basic assumptions

The geometrical relationships developed by Entwistle and White (1977) for the behaviour of the reinforcement before and after pressurisation have been taken as the basis for this current model. The geometry is shown in Fig. 1 and the geometrical relationships can be summarised by following expressions:

$$\varepsilon_i = (1+\varepsilon_z)\frac{\cos\alpha_i}{\cos\alpha_i'} - 1 \tag{13}$$

$$R_i' = R_i(1+\varepsilon_z)\frac{\tan\alpha_i'}{\tan\alpha_i} \tag{14}$$

This model assumes no twist of the hose on pressurisation. This is thought to be a reasonable simplification, since there is no noticeable twist of these hoses in experience (they are designed with layers of alternate direction). The torsional assumptions in the form derived by Breig (1988) are not included.

The definition of the winding radius of the various reinforcement layers and the inner core is taken to be the inner dimension. As there are no layers of rubber or plastic between reinforcement layers in the hose being modelled the expression within the axial equilibrium equation (Eq. (6)) relating to this has been dropped. Additionally the interlayer compatibility has been replaced by a new simple expression similar to that used by Jakeman and Knight (1995). The detailed expressions will be given in the following sections.

3.2. Inner core relationships

The well known theory of Lamé and Clapeyron (1833) for thick walled cylinder has been utilised. For the particular case of a cylinder loaded with internal and external pressure, expressions can be derived for the radial and hoop stresses (see for example Housner and Vreeland (1966)). Both expressions are a function of the radius r and are as follows:

$$\sigma_r = \frac{P_0R_0^2\left[1-\frac{R_1^2}{r^2}\right] - P_1R_1^2\left[1-\frac{R_0^2}{r^2}\right]}{[R_1^2-R_0^2]} \tag{15}$$

$$\sigma_\vartheta = -\frac{P_0R_0^2\left[1+\frac{R_1^2}{r^2}\right] - P_1R_1^2\left[1+\frac{R_0^2}{r^2}\right]}{[R_1^2-R_0^2]} \tag{16}$$

Using the generalised Hooke's law, an expression can also be derived for the axial stress and reduces to:

$$\sigma_z = E\varepsilon_z + v(\sigma_r+\sigma_\vartheta) = E\varepsilon_z + \frac{2v(P_0R_0^2 - P_1R_1^2)}{(R_1^2-R_0^2)} \tag{17}$$

This expression is not a function of radius and is constant across the cross-section of the cylinder. The axial force contribution of the inner core F_{zic}, is simply the axial stress multiplied by the deformed cross-sectional area of the cylinder i.e.:

$$F_{\text{zic}} = \sigma_z\pi(R_1'^2 - R_0'^2) \tag{18}$$

The hoop strain can be derived in terms of the stresses in the three cylindrical components and the elastic constants of the tube. As can be proved (Housner and Vreeland, 1966) the hoop strain is equal to the radial displacement, u, divided by the radius (i.e. u/r). Substituting the hoop, axial and radial stresses into the generalised Hooke's expression for hoop strain we gain an expression for u/r as follows:

$$\varepsilon_\vartheta = \frac{u}{r} = \frac{1}{E}\left[\frac{(R_0^2P_0 - R_1^2P_1)(1-v) + (P_0 - P_1)\frac{R_0^2R_1^2}{r^2}(1+v) - 2v^2(P_0R_0^2 - P_1R_1^2)}{R_1^2 - R_0^2} - vE\varepsilon_z\right] \tag{19}$$

For the specific case of $r = R_1$ then $u = R_1' - R_1$, substituting in these values and solving for P_1 we get the following expression:

$$P_1 = \frac{2(1-v_{ic})}{\left[1 + \frac{R_1^2(1-2v_{ic})}{R_0^2}\right]}\left[P_0 - \frac{E_{ic}(R_1^2 - R_0^2)}{2R_1R_0^2(1-v_{ic}^2)}(R_1' - R_1 + R_1v_{ic}\varepsilon_z)\right] \tag{20}$$

The expressions for F_{zic}, P_0 and P_1 are used later in the general model for the hose. It can be seen that if a Poisson's ratio, v, of 0.5 is substituted in Eq. (20) it reduces to the expression by Breig (1988) for P_0, i.e. Eq. (11). A further expression is required in order to relate the deformed internal radius of the core to the pressures, geometry and material properties. This is achieved by substituting the generalised Hooke's law with the internal boundary conditions, where $r = R_0$ and $u = R_0' - R_0$, after some algebraic manipulation the internal deformed radius R_0' is given by the following:

$$R_0' = \frac{R_0(1+v_{ic})}{E_{ic}(R_1^2 - R_0^2)}\left[P_0(R_0^2(1-2v_{ic}) + R_1^2) - 2P_1R_1^2(1-v_{ic})\right] + R_0(1 - v_{ic}\varepsilon_z) \tag{21}$$

3.3. Lateral compression of wires

3.3.1. Development of an explicit force–strain relationship

Radzimovsky (1953) developed expressions for stress, strain and change in distance between centres for the case of two cylinders pressed together with a line force.

The expression has been conveniently tabulated by Young (1989) and can be expressed in terms of a lateral strain ε_L, and once the appropriate substitutions are made it can be reduced into the following form:

$$\varepsilon_L = \frac{\delta d}{d} = \frac{2F_{LU}(1-v^2)}{d\pi E}\left[\frac{2}{3} + 2\ln\left[\frac{2d}{2.15\sqrt{\frac{F_{LU}d}{2E}}}\right]\right] \tag{22}$$

The expression in this form cannot be utilised in the theory because the force per unit length, F_{LU}, is needed and this parameter is embedded implicitly in the equation. A numerical technique has been used to gain an expression for the force per unit length by plotting the force per unit length divided by the wire diameter versus the strain. The behaviour is linear within the region of interest and has therefore been approximated using a linear least squares approximation of the curve, giving the following expression:

$$F_{LU} = 0.1895\varepsilon_{li}E_id_i \tag{23}$$

3.3.2. Component in hose axial equilibrium equation

The force, F_L, for a given length l can easily be extracted from Eq. (23) as:

$$\frac{F_L}{l} = 0.1895\varepsilon_{li}E_id_i \tag{24}$$

This relationship must now be converted into the relevant hose coordinate system in order that it can be incorporated into equilibrium equations. The geometrical configuration of the squeezing effect is shown graphically in Fig. 2.

The component, F_a, of the lateral force, F_L, that acts in the axial direction is given by:

$$F_a = F_L\sin\alpha_i' \tag{25}$$

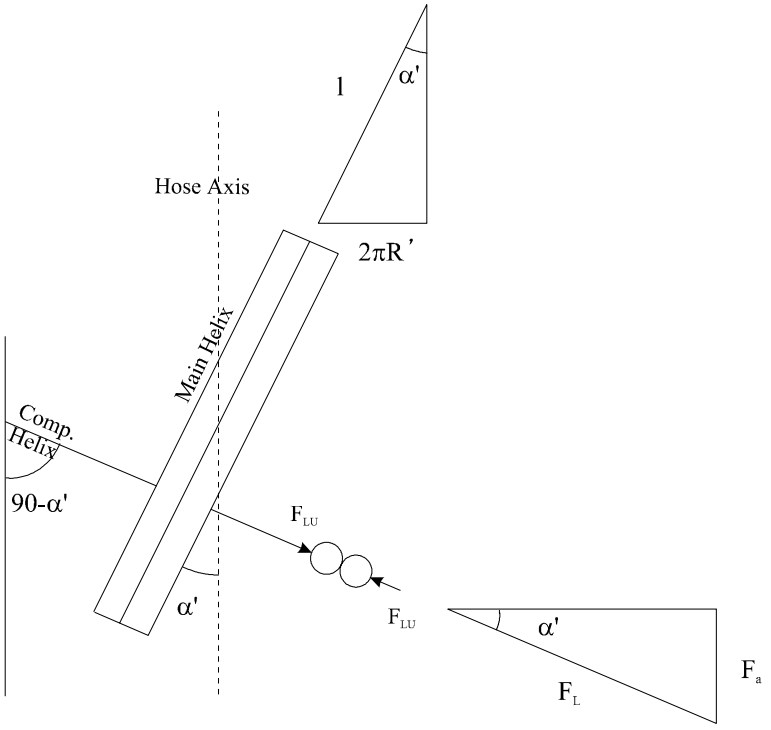

Fig. 2. The configuration of the wires pressed together with respect to the hose axis, and also the complementary helix angle.

and from Fig. 2 we have

$$\sin \alpha_i' = \frac{2\pi R_i'}{l} \tag{26}$$

Combining these two equations gives the following relationship:

$$\frac{F_{\mathrm{L}}}{l} = \frac{F_{\mathrm{a}}}{2\pi R_i'} \tag{27}$$

The length of wire which will contribute to this aspect of the axial force equation will be one pitch, as the wire within a pitch occupies different locations laterally and therefore will have a cumulative effect. After one pitch the wire will wrap back on itself and will not change the axial stiffness.

The calculation of the lateral strain acting on a wire in the ith layer is based on the following: the available space for a wire d_{sp} (see Fig. 3) can be calculated from the deformed hose geometry and the number of wires in a layer and can easily be shown to be the following relationship:

$$d_{\mathrm{sp}} = \frac{\cos \alpha_i' 2\pi \left[R_i' + \frac{d_i}{2}\right]}{N_i} \tag{28}$$

Clearly the lateral strain will only be non-zero if it is negative and it can be calculated from the following relationship:

$$\varepsilon_{\mathrm{l}i} = \frac{d_{\mathrm{sp}} - d_i}{d_i} \tag{29}$$

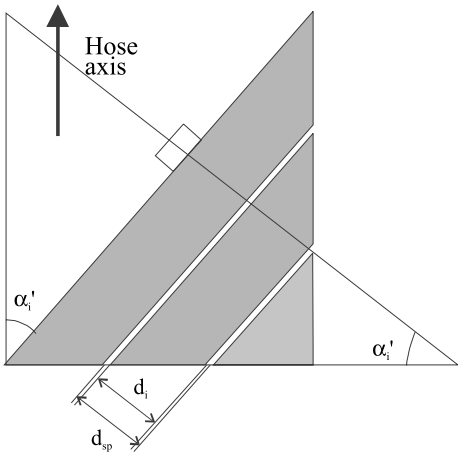

Fig. 3. The available space for a wire, d_{sp} compared with a wire diameter, d_i, for the case where $d_{sp} > d_i$, i.e $\varepsilon_{li} = 0$ and there will be no squeezing of wire.

Combining the above relationships we gain an expression for the axial force caused by the crushing effect on one layer of reinforcement as:

$$F_a = (0.1895)2\pi R'_i \varepsilon_{li} E_i d_i \tag{30}$$

In considering all layers the relationship must be made into a summation as follows:

$$F_a = (0.1895)2\pi \sum_{i=1}^{n} \xi_i[\varepsilon_{li}]_i R'_i \varepsilon_{li} E_i d_i \tag{31}$$

where for i is 1 to n and if $\varepsilon_{li} \geqslant 0$; $\xi_i[\varepsilon_{li}] = 0$ else $\xi_i[\varepsilon_{li}] = 1$.

A new series of factors are introduced at this point, $\xi_i[\varepsilon_{li}]$, these are switch variables, one for each layer. If the available space for the wire is less than the wire diameter, a crushing force will exist and the switch variable will be turned on (i.e. $\xi_i[\varepsilon_{li}], = 1$), if not there will be no squeezing effect and the switch variable will be turned off (i.e. $\xi_i[\varepsilon_{li}], = 0$).

3.3.3. Component in hose lateral equilibrium equation

The lateral squeezing effect on the wires will enable the wires to bear some of the pressure as a result of equilibrium considerations as shown in Fig. 4.

This effect can be incorporated into the lateral equilibrium equation. The pressure component of the squeezing effect can be calculated by means of the radius of curvature of its helix, however this effect runs perpendicular to the wire axis and therefore the radius of curvature will be the complimentary helix as shown in Fig. 2. The radius of curvature of the complimentary helix, ρ_c is given as:

$$\rho_c = \frac{R'_i}{\sin^2(90 - \alpha'_i)} = \frac{R'_i}{\cos^2 \alpha'_i} \tag{32}$$

The lateral pressure effect is then the force per unit length divided by the radius of curvature of the complimentary helix, i.e.:

$$P_L = \frac{F_{LU}}{\rho_c} \tag{33}$$

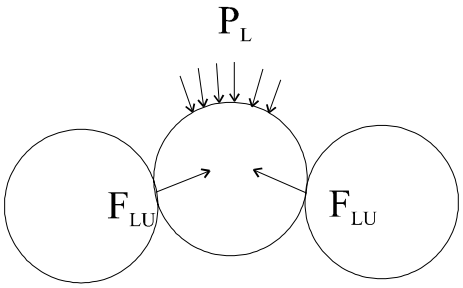

Fig. 4. The pressure caused by the compression of the wires together (note this is looking along the length of the wires and not the hose).

There is no need to obtain this expression in the hose axis as it is a pressure and would therefore be unchanged. Substituting Eqs. (23) and (32) into the previous expression and also substituting the expressions for R'_i (Eq. (14)) and ε_{li} (Eq. (29)) as well as adding the switch variables, ξ_i, we gain an expression for the pressure caused by the crushing effect on one layer as follows:

$$P_{\mathrm{L}} = \xi_i[\varepsilon_{li}]\left[\frac{(0.1895)\varepsilon_{li}E_i d_i \cos^2\alpha'_i}{R'_i}\right] \tag{34}$$

The difference in the interface pressures on the inside and outside of a layer can be equated to this crushing component added to a tension component (as given in Eq. (5) for all layers). Combining these pressure differences for all layers it is possible to equate the pressure on the inside of layer 1 to a summation of all the tension and crushing components of the layers in the hose (as is given in Eq. (36)). Extending this idea further it is possible to equate the interfacial pressure between any two layers to a summation of the crushing and tension expressions for the layers further out than the interface.

3.4. The general form of the equations

Having derived expressions for the aspects of the behaviour peculiar to the hose of current interest, it is now possible to give a new set of governing equations for a structural model. Firstly the axial equilibrium equation takes the form:

$$\pi R'^2_0 P_0 + F_{\mathrm{zic}} = \sum_{i=1}^{n} N_i A_i E_i \varepsilon_i \cos\alpha'_i + (0.1895)2\pi \sum_{i=1}^{n} \xi[\varepsilon_{li}] R'_i v_i \varepsilon_{li} E_i d_i \tag{35}$$

It is seen that it is the internal pressure multiplied by the end area of the hose plus an axial force component caused by the inner core, F_{zic} which has been derived and is given in Eq. (18). These are equated to the load bearing of the wires in the tension component, unchanged from the original Entwistle and White (1977) model (i.e. in Eq. (6)) added to the axial component of the squeezing effect as derived in the previous section. Note that the second expression on the right-hand side of the equation will always have the opposite sign to the first expression as it will only be non-zero when $\varepsilon_{li} < 0$. The units for this equation are force (N).

The lateral equilibrium equation is in the form:

$$P_{\mathrm{l}} = \sum_{i=1}^{n} \frac{N_i A_i E_i \varepsilon_i \sin\alpha'_i \tan\alpha'_i}{2\pi R'^2_i} + \sum_{i=1}^{n} \xi_i \frac{(0.1895)\varepsilon_{li} E_i d_i \cos^2\alpha'_i}{R'_i} \tag{36}$$

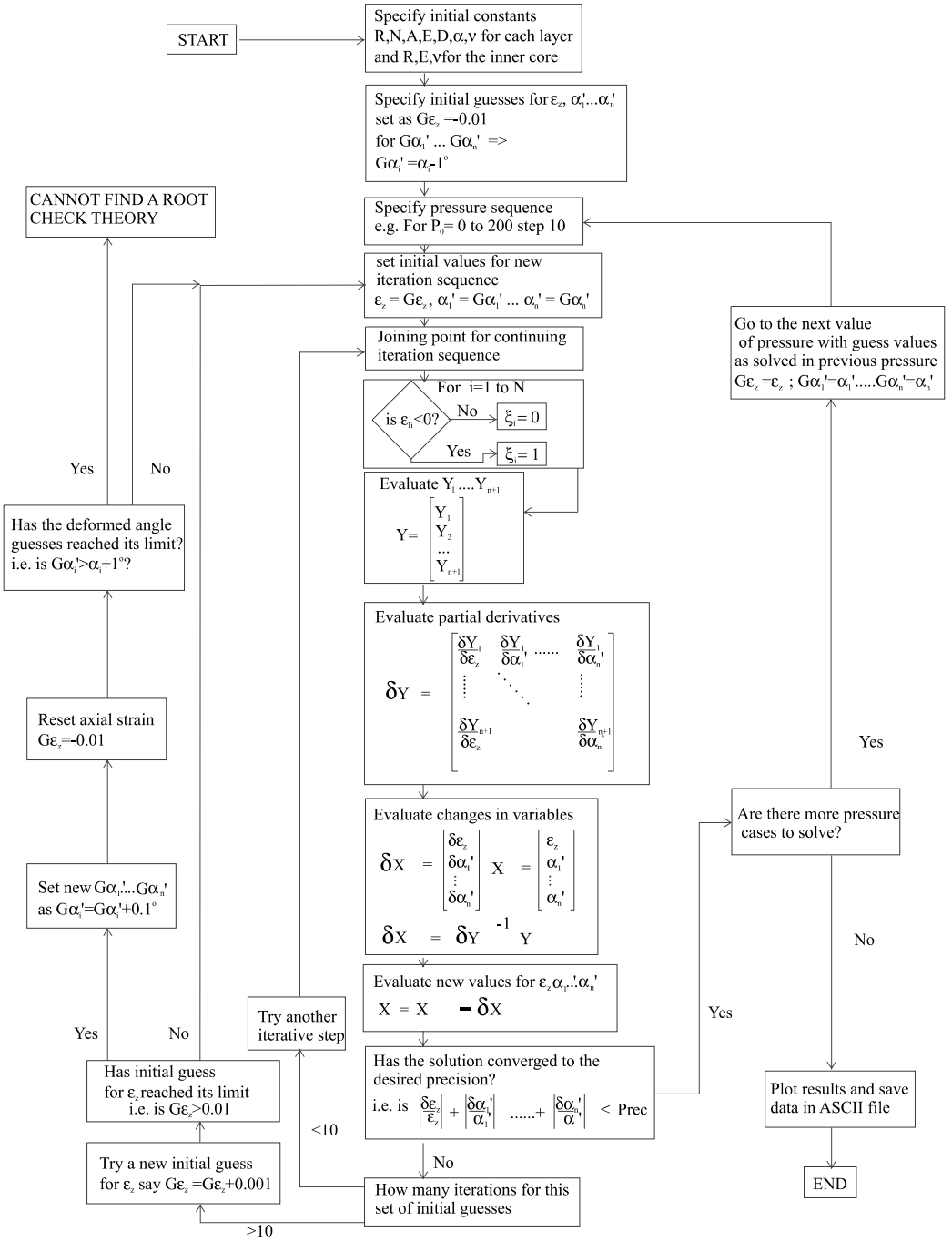

Fig. 5. Flow chart for numerical method.

It equates the interfacial pressure between the outside of the inner core and the first layer of reinforcement, i.e. P_1 (this has been derived in terms of the internal pressure P_0 in Eq. (20)). This is equated to

the pressure bearing of the wires acting in tension as proposed by Entwistle and White (1977) (as shown in Eq. (5)) added to the pressure bearing component borne by the wires when they are put under lateral compression as derived in the previous section. The units of this equation are pressure (i.e. N/mm^2).

The interlayer compatibility of the wires has been approximated by a similar assumption to that used by Jakeman and Knight (1995) and is as follows:

$$R'_i + d_i = R'_{i+1} \tag{37}$$

for $i = 1$ to $n - 1$

The change of $2d_i$ to d_i is because this is a helical wound hose which has a layer thickness of d_i compared to a braided hose which has a layer thickness of $2d_i$. The units of the equation are length (mm) and there will be one equation for every interlayer existing, i.e. $n - 1$ in a hose with n layers.

These expressions above are manipulated into a numerically solvable form, eliminating ε_i and R'_i (using Eqs. (13) and (14)). P_1 and R'_0 can also be substituted (Eqs. (20) and (21)) but since they equate to lengthy algebraic terms they are left as function substitutions. Each equation has been equated to a new variable, Y_i. This new series of variables allows a minimising technique to be used in a numerical solution. There are $n + 1$ equations and $n + 2$ unknowns which are the n winding angles after pressurisation, α'_i, the axial hose strain, ε_z, and the internal pressure P_0. Since the solution is generally sought for a given pressure this leaves $n + 1$ unknowns and the solution is therefore feasible. It is not possible to manipulate these equations into a closed form solution and a numerical technique must be used to reach a solution.

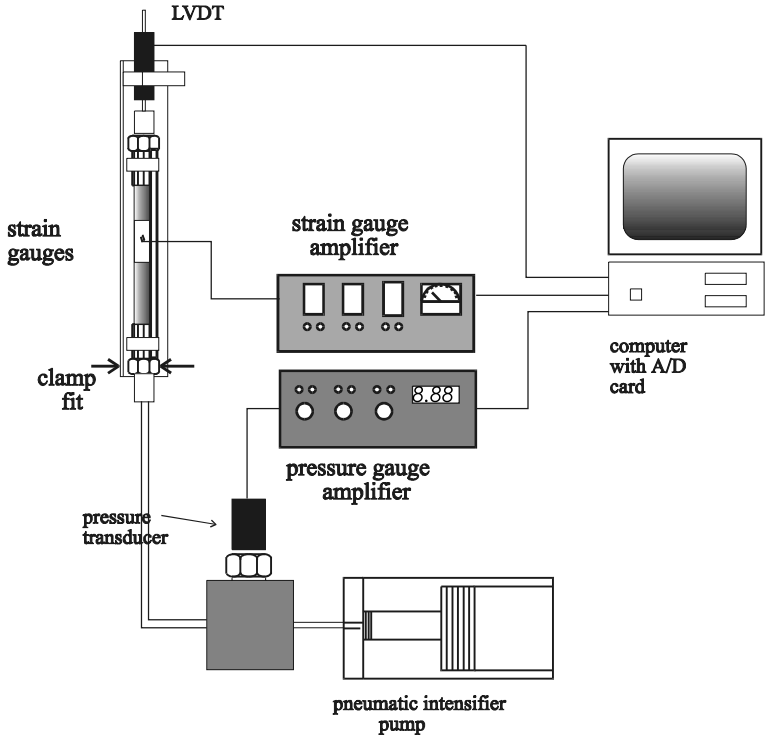

Fig. 6. Schematic view of the experimental test set-up for hose assembly tests.

3.5. Numerical solution

The solution to the equations is found using a minimising Newton Raphson technique (Ortega and Rheinboldt, 1970) implemented in Matlab on a Pentium 200 PC. The solution is not guaranteed to converge, it may converge to a local inflexion or may diverge. One advantage in this particular problem is that fairly good initial estimates for variables can be made. Generally it was found that if a solution did not converge within 10 cycles it was probably drifting off to a root with no physical meaning. It was found in some cases that the initial estimate was critical as to whether the solution was going to converge or not, hence if it had not converged within 10 cycles the initial estimates were changed and the iteration repeated. In this way the full range and combination of likely roots could be tried and this technique worked well for the few situations which were very sensitive to the initial estimated values. For the majority of cases however the iteration was relatively robust and not very sensitive to the initial values input. Once the first pressure case had been solved the solution to the variables was then used as the estimate for the next pressure case and often this resulted in a convergence within three cycles. The solution to a complete hose pressure region, even for most complex hose, solving for 50 pressure points, does not take more than a few minutes. A flow chart for the numerical technique is given in Fig. 5. The partial derivatives for the solution were calculated symbolically and checked with a simple numerical approximation.

4. Experimental technique

The basic experimental set-up is shown in Fig. 6. The hose was pressurised using a hydraulic pump driven pneumatically by line pressure. The pump was capable of delivering pressures up to 2759 bar (40,000 PSI)

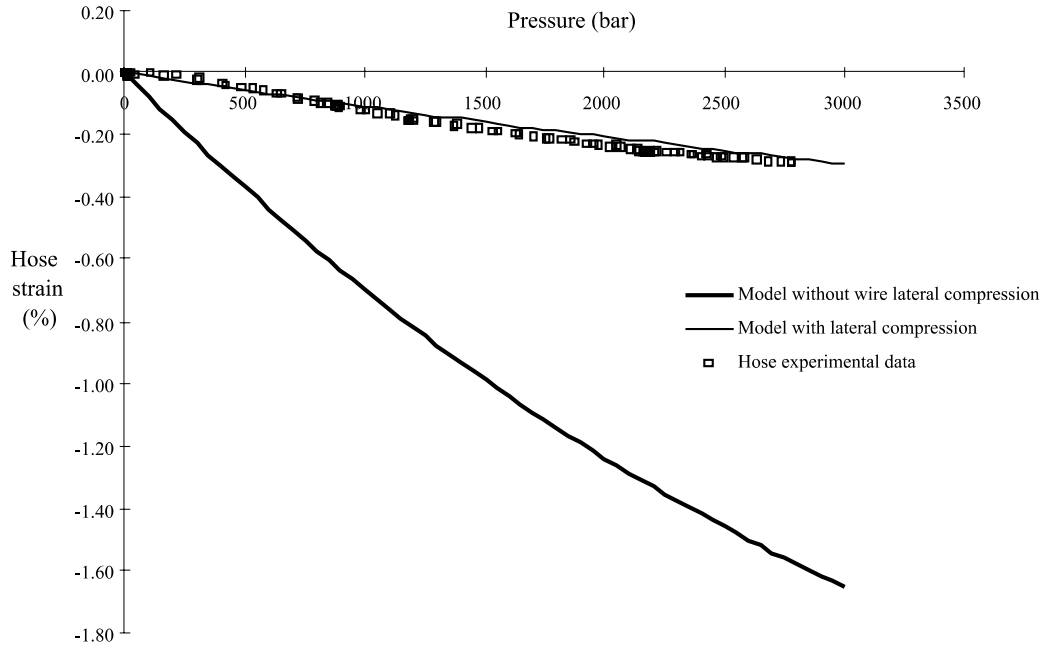

Fig. 7. An example of a hose behaviour compared with model predictions from the model which incorporates wire squeezing to the model that ignores it (6005st).

by nature of being an intensifier, i.e. with a step down large to small diameter on the main piston. The hose was connected to the pump by means of a manifold, which allowed the connection of a pressure transducer, Bourdon pressure gauge and a pressure release valve. The connection between the hose and test rig was an autoclave fitting utilising 60° cone to cone sealing line contact. The other end of the hose was plugged with a blank version of the same fitting.

On the plugged end of the hose a linear variable differential transformer (LVDT) was used to monitor the axial displacements. The LVDT gave an output which was amplified to a signal between 0 and 6 V and channelled into the computer with an A/D card. In the centre of the hose a section of the outer cover was stripped off to expose the outer reinforcement wires. These were then cleaned and treated to allow small strain gauges to be attached along the axis of the wires. Single strain gauges were used in a quarter bridge configuration and amplified (Micro Measurements 2120) before the signals were also fed into the data acquisition computer via the A/D card.

Keeping the hose straight under pressurisation was difficult because of the slightly curved nature of the hose caused by being stored on a reel. For this reason it was found necessary to strap the hose to a steel angle iron by means of a number of lubricated rubber straps. More details on the experimental technique can be found in the thesis of the first author (Evans, 1999).

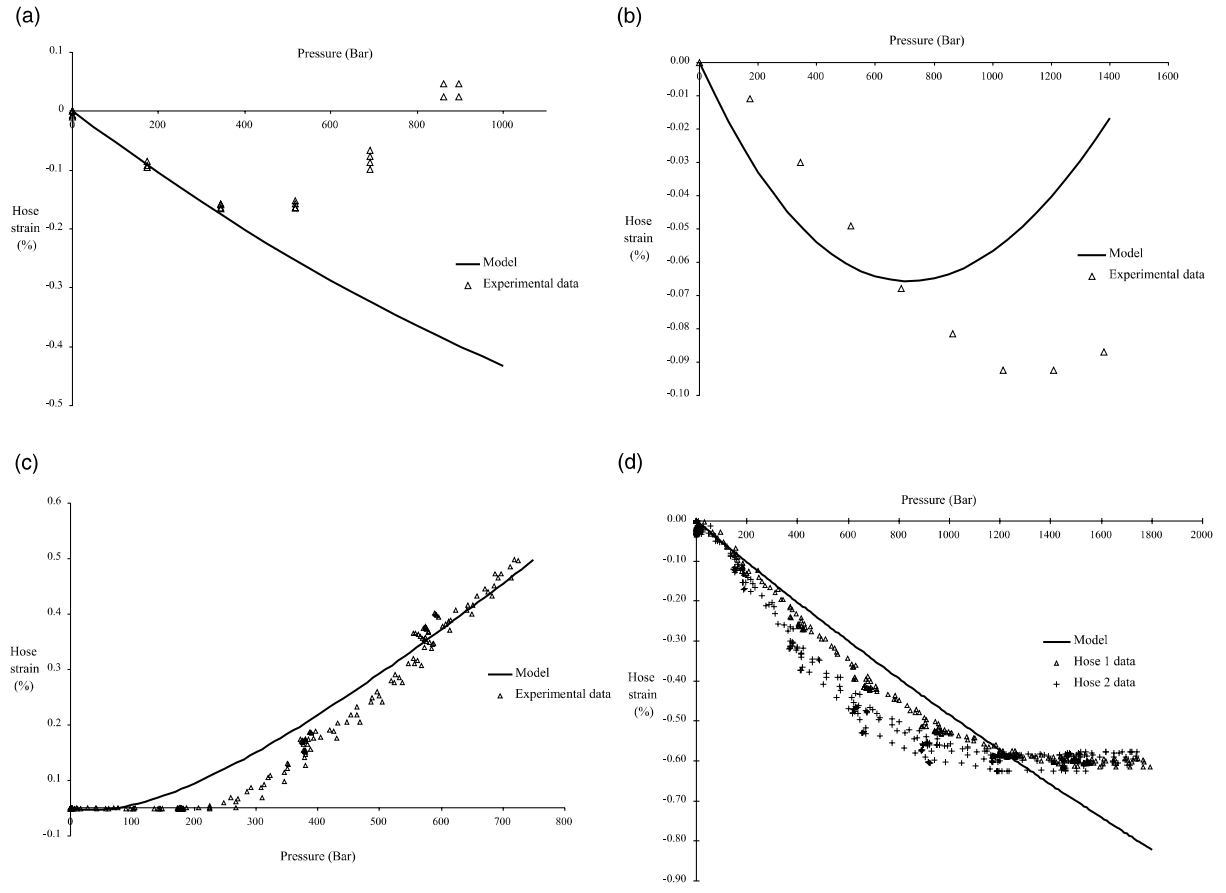

Fig. 8. Pressure versus hose axial strain response compared with model predictions for the following hoses: (a) 2006st, (b) 2006str, (c) 2012st and (d) 4012st.

5. Comparison of predictions with experimental results—discussion

Fig. 7 gives an example of experimental results for length change compared with two model predictions: the current model incorporating wire lateral compression and the original model i.e., a version of Entwistle and White (1977). There is a significant difference between the predictions with the current model much closer to the experimental data. The original model predictions have been omitted from the rest of the results as they vary from experimental results to a similar level as seen in Fig. 7.

Figs. 8 and 9 show the length change of all the hoses tested in this work compared with predictions from the model. Hose 2012 (Fig. 8(c)), is the only hose that gets longer, from the tests carried out. There appears to be good agreement between experimental results and theoretical predictions for hose length change. Where the hose gets shorter the behaviour tends to show a gradually decreasing pressure strain gradient whereas the model tends to predict a more linear response. The reason for this difference could be caused by the extrusion of the core material into the first layer of wires, which has the effect of increasing the axial load on the hose. This effect has not been incorporated into the model. One hose (6012st Fig. 9(c)) shows some difference between the model and experimental results, the model predicting a smaller length change than actually measured. The reason for this is not known but may be caused by the wires in one or more

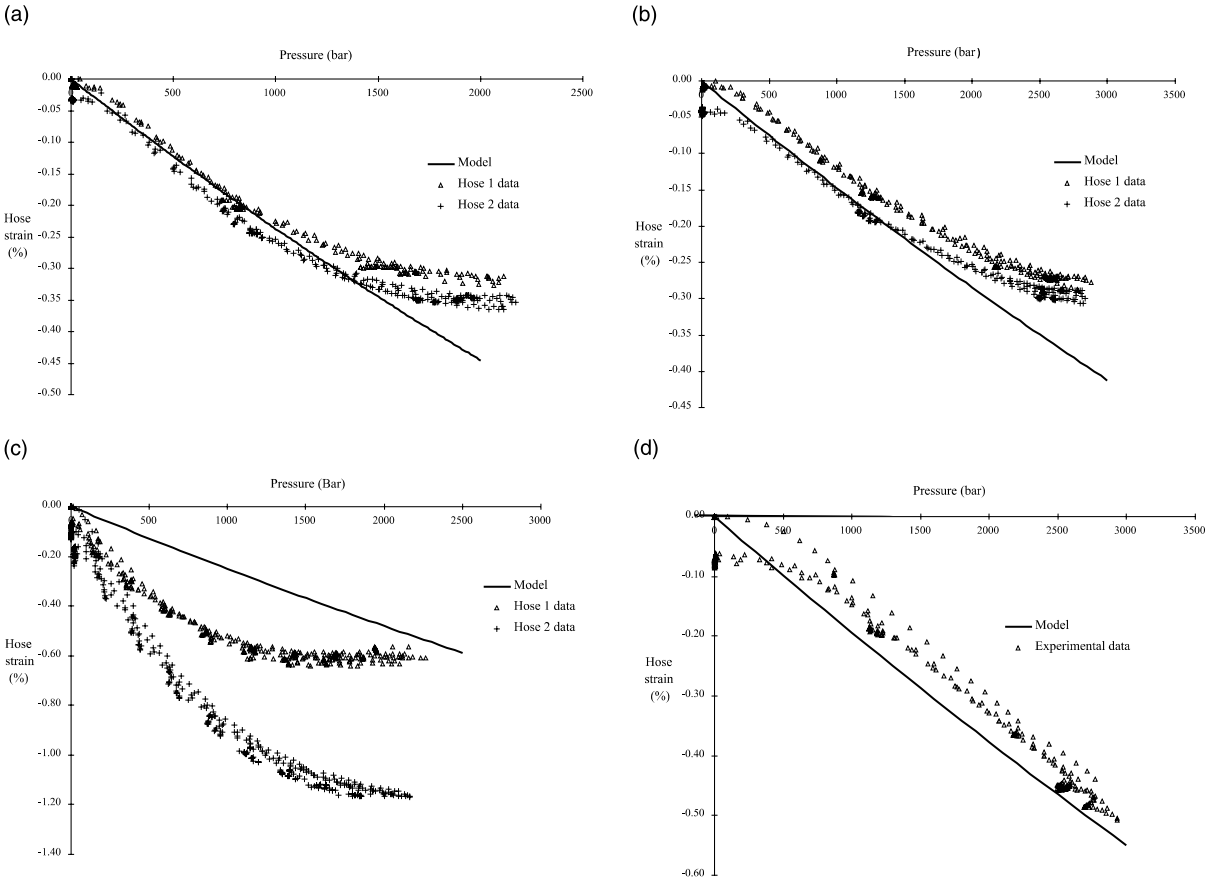

Fig. 9. Pressure versus hose axial strain response compared with model predictions for the following hoses: (a) 4006st, (b) 6005st, (c) 6012st and (d) 8005st.

layers not completely touching. In this case the length change may be a good indicator of the hose manufacturing quality in terms of wire packing density. In one case (hose 2006str Fig. 8(b)) a reversal in the direction of strain is seen both experimentally and in the predicted results. This can be explained the simple 'neutral angle' idea (see for example Evans (1974)). Initially as the hose is getting shorter the wires are realigning towards an equilibrium point, once reached the hose acts like a solid pipe and gets longer and wider according to normal continuum theory.

Fig. 10(a) and (b) gives two examples of the significant levels of hysteresis seen in the axial response of all the hoses investigated. This is likely to be caused by frictional forces at points of contact between wires in alternate layers and line contacts between wires in the same layers. As the hose changes in length there will be a rotation around the point contacts and translational movements between the line contacts in wires in the same layer. These movements will be inhibited by frictional effects and this would also account for the heating up of the hose during fatigue testing. The level of hysteresis may be a good method of gaining an insight into the relative motion between layers of reinforcement caused by pressure cycling. Clearly hysteretic loss will be a function of both interlayer pressure and motion and given that fretting of wires is dependant among other things on stress and motion between contacting wires, then hysteresis might correlate with the likely degree of fretting, The contribution of the polymeric components of the hose to the hysteretic behaviour will be relatively small as these are highly deformable elastic materials in comparison to the very stiff wires.

Fig. 11 shows the pressure versus wire strain behaviour and a comparison with the model prediction. The predicted and measured wire strains show, excellent agreement. The measured results in the majority of cases show a linear response, the two exceptions to this were on hose 4012st and hose 4006st (Fig. 11(a) and (b)). For these hoses in both cases tests at two locations were carried out, one result shows a linear response and agrees with the model, while the second shows a lower strain response and a gradual increase in gradient towards a linear response. One explanation of this is that the non-linear behaviour is that of a slacker wire. When wires are wound onto the hose the winding drums are controlled with a friction brake. During a down period of a particular hose winding machine a spring balance was used to gain an indication of the variation in braking force between different spools. In the tests carried out a wide variation (around

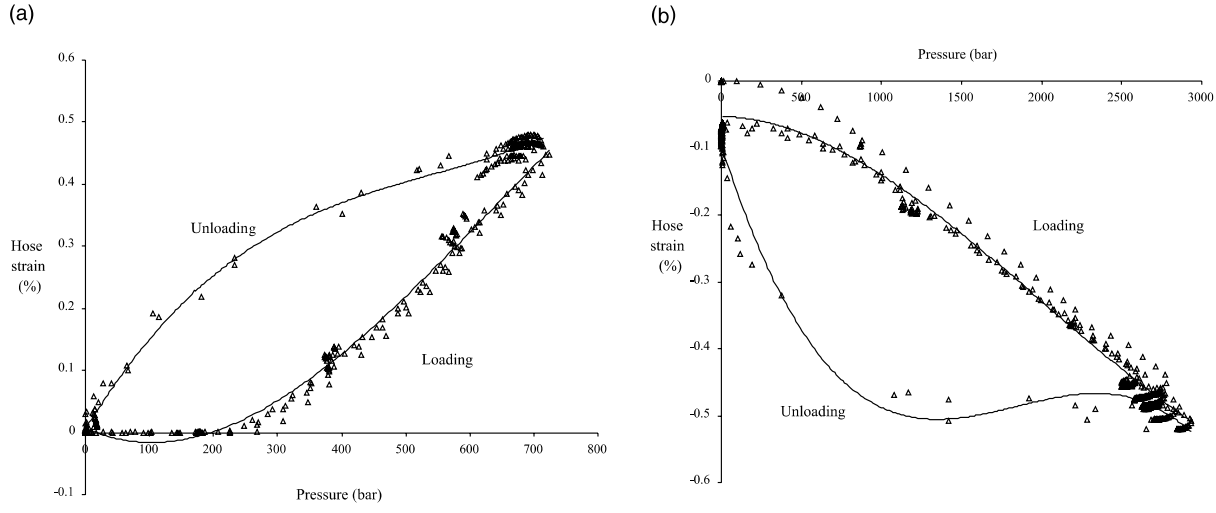

Fig. 10. Two examples of hysteresis seen in hose length change during pressure cycling, (a) for hose getting longer (2012st) and (b) for hose getting longer (8005st).

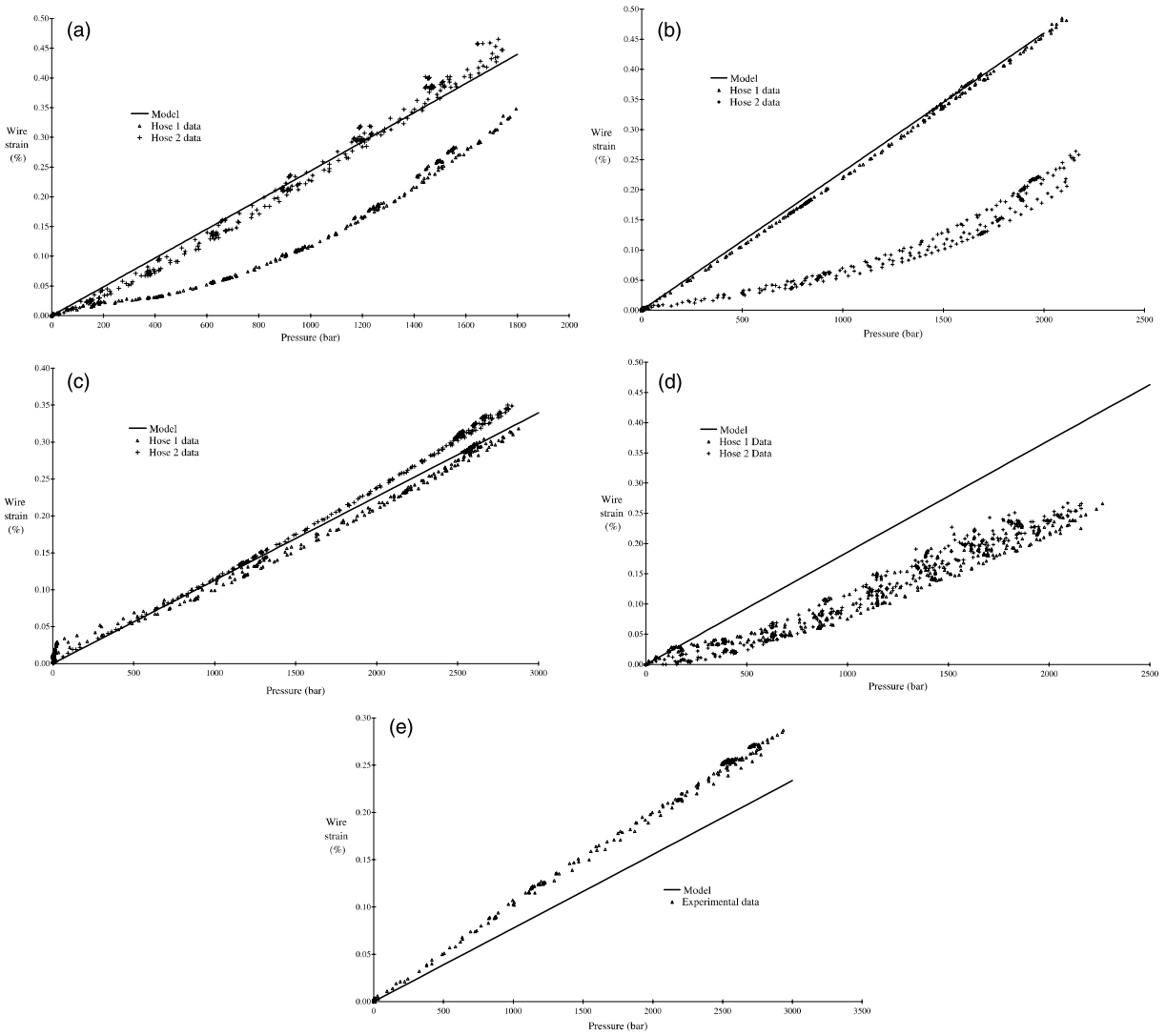

Fig. 11. Pressure versus wire strain response compared with model predictions for the following hoses: (a) 4012st, (b) 4006st, (c) 6005st, (d) 6012st and (e) 8005st.

75% of mean) was recorded. It may be that the spool tension must go beyond some threshold level in order to avoid a slack wire problem.

6. Conclusions

The model presented shows good agreement with experimental results and may be used by hose designers to predict hose behaviour and improve hose performance. In addition to predicting hose length

change and wire tensions it can also predict the wire angle change and radial strain. The current model does not attempt to model the axial hysteresis in the hose and this could be an interesting topic for future work.

Acknowledgements

Polyflex GmbH provided hose samples and financial support for the work. Alex Noorbai, Nick Taylor, Mark Evans and Shi Chi Hos helped set experimental work up. Thanks to J.H. Evans, D.K. Longmore and J.A. Witz for reading the work and giving many useful suggestions.

References

Anon, 1992. Polyflex High Pressure Hoses-Product Catalogue. Polyflex Gmbh, Huttenfeld, Germany.

Breig, W.F., 1988. Mathematical and experimental pressure-deformation response of helically wound wire reinforced elastomeric hose. SAE Technical Paper Series (881301.), 6.1593–6.1607.

Cardou, A., Jolicoeur, C., 1997. Mechanical models of helical strands. Applied Mechanics Reviews 50 (1), 1–14.

Entwistle, K.M., White, G.W., 1977. A method for achieving effective load transfer between the inner and outer layers of a two-layer braided high pressure hydraulic hose. International Journal of Mechnical Science 19, 193–201.

Evans, C.W., 1974. Hose Technology. Applied Science Publishers, Barking.

Evans, J.J., 1999. Aspects of the mechanical behaviour of helical wire structures relating to quasi static and fatigue properties. Department of Mechanical Engineering, Imperial College, London, p. 242.

Housner, G.W., Vreeland, T., 1966. The Analysis of Stress and Deformation. Collier–Macmillan, London.

Hruska, F., 1952. Radial forces in wire ropes. Wire and Wire Products 27 (5), 459–463.

Hruska, F., 1953. Tangential forces in wire ropes. Wire and Wire Products 28 (5), 455–460.

Hruska, F.H., 1951. Calculation of stresses in wire ropes. Wire (September), 766–801.

Jakeman, R.R., Knight, P.H., 1995. Development of a High Pressure Thermoplastic Hose. Umbilicals: The Future. Society for Underwater Technology.

Knapp, R.H., 1979. Derivation of a new stiffness matrix for helically armoured cables considering tension and torsion. International Journal for Numerical Methods in Engineering 14, 515–529.1.

Kuipers, M., Veen, M., 1989. On stresses in reinforced high pressure hoses. Acta Mechanica 80, 313–322.

Lamé, G., Clapeyron, B.P.E., 1833. Mémoire présentés par Divers Savants. Paris.

Lord, E.A., Wilson, C.B., 1984. The Mathematical Description of Shape and Form. Ellis Horwood, West Sussex.

Machida, S., Durelli, A.J., 1973. Response of a strand to axial and torsional displacements. Journal of Mechanical Engineering Science 15 (4), 241–251.

Ortega, J.M., Rheinboldt, W.C., 1970. Iterative Solution to Nonlinear Equations in Several Variables. Academic Press, New York.

Radzimovsky, E.I., 1953. Stress distribution and strength conditions of two rolling cylinders pressed together. Engineering Experiment Station, University of Illinois, p. 408.

Raghaven, C., Olsen, J., 1989. Development of a 7000 bar hose. 5th American Water Jet Conference, Toronto, USWJTA.

SAE J517, 1986. Hydraulic Hose.

Teerling, H.L.J., 1994. Strength and Stiffness of High Pressure Hoses (Ph.D. thesis in English). Wiskunde en Natuurwetenschappen. Rijksuniversiteit Groningen, Groningen, 150pp.

Van Den Horn, B.A., Kuipers, M., 1988. Strength and stiffness of a reinforced flexible hose. Applied Scientific Research 45, 251–281.

Young, W.C., 1989. Roark's Formulas for Stress and Strain. McGraw-Hill, New York.